



Three trinuclear Ru(II) complexes containing 4,5-diazafluorene and 2,2'-bipyridine: synthesis, absorption spectrum, luminescence, and redox behavior

Feixiang Cheng, Chixian He, Lifeng Yao, Fan Wang & Ning Tang

To cite this article: Feixiang Cheng, Chixian He, Lifeng Yao, Fan Wang & Ning Tang (2015) Three trinuclear Ru(II) complexes containing 4,5-diazafluorene and 2,2'-bipyridine: synthesis, absorption spectrum, luminescence, and redox behavior, Journal of Coordination Chemistry, 68:4, 704-716, DOI: [10.1080/00958972.2014.994512](https://doi.org/10.1080/00958972.2014.994512)


To link to this article: <http://dx.doi.org/10.1080/00958972.2014.994512>

 View supplementary material [↗](#)

 Accepted author version posted online: 08 Dec 2014.
Published online: 02 Jan 2015.

 Submit your article to this journal [↗](#)

 Article views: 63

 View related articles [↗](#)

 View Crossmark data [↗](#)

 Citing articles: 1 View citing articles [↗](#)

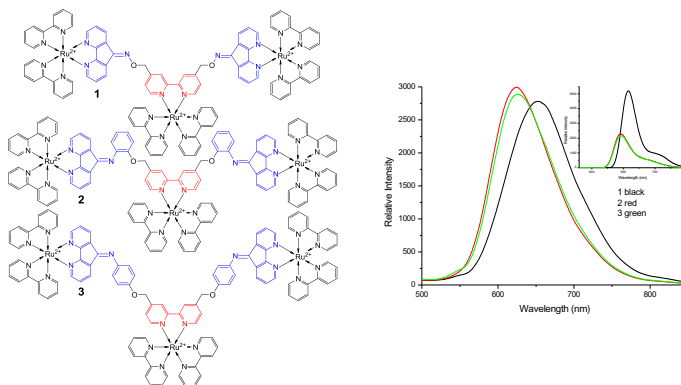
Three trinuclear Ru(II) complexes containing 4,5-diazafluorene and 2,2'-bipyridine: synthesis, absorption spectrum, luminescence, and redox behavior

FEIXIANG CHENG*[†], CHIXIAN HE[‡], LIFENG YAO[†], FAN WANG[†] and NING TANG[‡]

[†]College of Chemistry and Chemical Engineering, Qujing Normal University, Qujing, PR China

[‡]College of Chemistry and Chemical Engineering, Lanzhou University, Lanzhou, PR China

(Received 9 April 2014; accepted 10 November 2014)



Three heterotopic ligands L^1 , L^2 , and L^3 have been prepared by the reaction of 4,4'-bis(bromomethyl)-2,2'-bipyridine with 4,5-diazafluoren-9-oxime, 9-(2-hydroxy)phenylimino-4,5-diazafluorene, and 9-(4-hydroxy)phenylimino-4,5-diazafluorene, respectively, in DMF. The three ligands consist of two 4,5-diazafluorene units and one 2,2'-bipyridine unit. Ru(II) complexes $[\{Ru(bpy)_2\}_3(\mu_3-L^{1-3})](PF_6)_6$ (bpy = 2,2'-bipyridine) were prepared by refluxing $Ru(bpy)_2Cl_2 \cdot 2H_2O$ and the ligands in 2-methoxyethanol. The three Ru(II) complexes display metal-to-ligand charge-transfer absorption at 445–450 nm and one Ru(II)-centered oxidation at 1.32 V in CH_3CN solution at room temperature. Upon excitation into the metal-to-ligand charge-transfer band, the emission intensities of $[\{Ru(bpy)_2\}_3(\mu_3-L^2)]^{6+}$ and $[\{Ru(bpy)_2\}_3(\mu_3-L^3)]^{6+}$ are almost equal to that of $[\{Ru(bpy)_2\}_3(\mu_3-L^1)]^{6+}$ in CH_3CN solution at room temperature, but weaker than that of $[\{Ru(bpy)_2\}_3(\mu_3-L^1)]^{6+}$ in EtOH–MeOH (4 : 1, v/v) glassy matrix at 77 K.

Keywords: Ru(II) complex; Heterotopic ligand; Photophysics; Electrochemistry

*Corresponding author. Email: chengfx2010@163.com

1. Introduction

Polynuclear complexes capable of performing effective light-induced functions require the availability of molecular components having suitable chemical properties and structures [1–3]. Ru(II) polypyridyl complexes are extensively used as building blocks for the construction of such devices because of their outstanding electrochemical and photophysical properties [4–7]. The efficiency of photoactive processes in polynuclear complexes is strongly regulated by the size, shape, and electronic nature of the bridging ligands [8–10]. The shape and structure of the bridging ligand controls the structure of the supramolecular system, i.e. the overall arrangement of the individual components; the nature of the groups linking the binding sites controls the extent of electronic communication between the building blocks. Therefore, the bridging ligands that connect two or more metal polypyridine subunits are crucial to obtain polynuclear complexes capable of exhibiting interesting photophysical and electrochemical properties, and of giving photoactive processes. Bridging ligands containing bidentate ligands such as 2,2'-bipyridine or 1,10-phenanthroline and their derivatives as chelating units, have been prepared. However, the vast majority of such studies have focused on systems containing symmetric bridging ligands. The study of polynuclear Ru(II) complexes, bridged with heterotopic polypyridine ligands, has attracted less attention [11–18]. Coronado *et al.* reported a dinuclear complex [Ru(bpy)₂(PT)Ru(tpy)] [PF₆]₄ containing a heterotopic phenanthroline–terpyridine bridging ligand. Emission studies indicate an energy transfer from the Ru(bpy)₂(PT) moiety to the (PT)Ru(tpy)'s center [17]. Mesmaeker *et al.* reported two tetranuclear Ru(II) polypyridine complexes based on the heterotopic bridging ligand PHENAT. Internal energy transfer takes place from the core to the peripheral metallic units in both the complexes [18].

4,5-Diazafluorene-9-one (dafone) is structurally similar to bpy and phen. However, the rigid structure imposed by the central five-membered ring means that the two nitrogens are always held in the same direction to avoid rotational conformation problems. Dafone has a much larger chelate bite than bpy and phen (N···N: dafone, 3.00 Å; bpy, 2.62 Å; phen, 2.64 Å). 4,5-Diazafluorene can selectively perturb the energy of ligand field (LF) states while leaving metal-to-ligand charge-transfer (MLCT) states nearly unchanged for Ru(II) diimine complexes. As a consequence, Ru(II) complexes including dafone have different photophysical and electrochemical properties from the Ru(bpy)₃²⁺ and Ru(phen)₃²⁺ based complexes [19, 20]. In an attempt to obtain more insight into the interesting photophysical and electrochemical properties of Ru(II) complexes with heterotopic bridging ligands, one interesting possibility is to combine 4,5-diazafluorene and 2,2'-bipyridine in a system. Based on the above arguments, we synthesized three heterotopic bridging ligands containing two kinds of non-equivalent chelating sites: one involving the 2,2'-bipyridine moiety and the other involving the 4,5-diazafluorene moiety. The photophysical and redox properties of the three complexes are discussed. Theoretical calculations of highest occupied molecular orbital (HOMO) and lowest lying unoccupied orbitals (LUMOs) for the three bridging ligands are also presented.

2. Experimental

2.1. Materials

2,2'-Bipyridine, 1,10-phenanthroline, 4-aminophenol, 2-aminophenol, 2,2'-bipyridine-4,4'-dimethanol, tetrabutylammonium perchlorate (TBAP), K₂CO₃, NH₂OH·HCl, RuCl₃·3H₂O,

NH_4PF_6 , CH_3CN , EtOH, MeOH, CH_2Cl_2 , DMF, petroleum, and ethyl acetate were purchased from the Tianjin Chemical Reagent Factory. Solvents and raw materials were of analytical grade and used as received, apart from CH_3CN , which was filtered over activated alumina and distilled from P_2O_5 immediately, prior to use. 4,5-Diazafluoren-9-oxime, 9-(2-hydroxy)phenylimino-4,5-diazafluorene, 9-(4-hydroxy)phenylimino-4,5-diazafluorene [21, 22], 4,4'-bis(bromomethyl)-2,2'-bipyridine [23], and $\text{Ru}(\text{bpy})_2\text{Cl}_2 \cdot 2\text{H}_2\text{O}$ [24] were synthesized according to literature procedures.

2.2. Physical measurements

^1H NMR spectra were recorded on a Mercury Plus 400 spectrometer using TMS as internal standard. ESI-MS spectra were obtained on a Bruker Daltonics Esquire 6000 mass spectrometer. Elemental analysis was taken using a Perkin-Elmer 240C analytical instrument and infrared spectra with a Thermo Nicolet AVATAR 360 FT-IR spectrometer. Absorption spectra were obtained on a Varian Cary-100 UV-visible spectrophotometer and emission spectra with a Hitachi F-4600 spectrophotometer. The emission quantum yields were calculated relative to $\text{Ru}(\text{bpy})_3^{2+}$ ($\Phi_{\text{std}} = 0.062$) in deoxygenated CH_3CN solution at room temperature [25] and relative to $\text{Ru}(\text{bpy})_3^{2+}$ ($\Phi_{\text{std}} = 0.376$) in EtOH–MeOH (4 : 1, v/v) glassy matrix at 77 K [26]. Cyclic voltammetry and differential pulse voltammetry were performed at room temperature using a CHI 660D electrochemical workstation. A standard three-electrode setup was used, consisting of a platinum disk working electrode, a platinum auxiliary electrode, and a saturated potassium chloride calomel reference electrode. Complexes were dissolved in distilled CH_3CN with 0.1 M L^{-1} TBAP as the supporting electrolyte.

2.3. Preparations

4,4'-Bis[(4,5-diazafluoren-9-ylimino)methyl]-2,2'-bipyridine (L^1): A mixture of 4,4'-bis(bromomethyl)-2,2'-bipyridine (213 mg, 0.63 mM), 4,5-diazafluoren-9-oxime (383 mg, 1.94 mM), and K_2CO_3 (337 mg, 2.44 mM) in DMF (30 mL) was heated to 90 °C for 48 h under nitrogen. The solution was poured into water (300 mL) after cooling to room temperature, and a white precipitate which formed was collected by filtration. The crude product was chromatographed on silica, being eluted first with CH_2Cl_2 –ethyl acetate (2 : 1, v/v) to remove impurities, then with CH_2Cl_2 –EtOH (25 : 1, v/v) to afford the desired product as a white solid. Yield: 149 mg (41.39%). ^1H NMR (400 MHz, CDCl_3): $\delta = 5.58$ (s, 4H), 7.29 (dd, $J = 7.6, 5.2$ Hz, 2H), 7.34 (dd, $J = 7.6, 5.2$ Hz, 2H), 7.43 (dd, $J = 5.2, 1.6$ Hz, 2H), 8.06 (dd, $J = 7.6, 1.6$ Hz, 2H), 8.52 (s, 2H), 8.57 (dd, $J = 7.6, 1.6$ Hz, 2H), 8.70 (d, $J = 4.8$ Hz, 2H), 8.72 (dd, $J = 4.8, 1.6$ Hz, 2H), 8.75 (dd, $J = 5.2, 1.6$ Hz, 2H). ESI-MS: $m/z = 575.3$ ($\text{M} + \text{H}$) $^+$, 597.3 ($\text{M} + \text{Na}$) $^+$. Anal. Calcd for $\text{C}_{34}\text{H}_{22}\text{N}_8\text{O}_2$ (%): C, 71.1; H, 3.9; N, 19.5. Found: C, 71.3; H, 4.1; N, 19.7. IR ν_{max} (KBr, cm^{-1}): 3426 (br), 1599s, 1563s, 1452m, 1397s, 1357w, 1288w, 1212w, 1164w, 1110w, 1048m, 1024s, 983s, 922w, 817m, 749s, 626w, 505w.

4,4'-Bis[2-(4,5-diazafluoren-9-ylimino)phenoxy]methyl]-2,2'-bipyridine (L^2): L^2 was prepared by the same procedure as that described for L^1 , except 9-(2-hydroxy)phenylimino-4,5-diazafluorene (481 mg, 1.76 mM) was used instead of 4,5-diazafluoren-9-oxime to react with 4,4'-bis(bromomethyl)-2,2'-bipyridine (187 mg, 0.55 mM). Yield: 145 mg (36.25%) of a red solid. ^1H NMR (400 MHz, CDCl_3): $\delta = 5.30$ (s, 4H), 6.92–6.99 (m, 6H), 7.05–7.10 (m, 4H), 7.20 (td, $J = 8.0, 1.6$ Hz, 2H), 7.36 (dd, $J = 7.6, 5.2$ Hz, 2H), 8.12 (s, 2H), 8.30

(dd, $J = 7.6, 1.6$ Hz, 2H), 8.35 (d, $J = 5.2$ Hz, 2H), 8.58 (dd, $J = 4.8, 1.6$ Hz, 2H), 8.76 (dd, $J = 4.8, 1.6$ Hz, 2H). ESI-MS: $m/z = 727.4$ (M + H)⁺. Anal. Calcd for C₄₆H₃₀N₈O₂ (%): C, 76.0; H, 4.2; N, 15.4. Found: C, 76.3; H, 4.4; N, 15.7. IR ν_{\max} (KBr, cm⁻¹): 3426 (br), 1660m, 1594s, 1564s, 1482s, 1451m, 1398s, 1248s, 1161w, 1106m, 1040w, 1004w, 947w, 825m, 754s, 709w, 631w, 510w.

4,4'-Bis[4-(4,5-diazafluoren-9-ylimino)phenoxyethyl]-2,2'-bipyridine (L³): L³ was prepared by the same procedure as that described for L¹, except 9-(4-hydroxy)phenylimino-4,5-diazafluorene (438 mg, 1.60 mM) was used instead of 4,5-diazafluoren-9-oxime to react with 4,4'-bis(bromomethyl)-2,2'-bipyridine (162 mg, 0.48 mM). Yield: 115 mg (33.24%) of a red solid. ¹H NMR (400 MHz, CDCl₃): $\delta = 5.27$ (s, 4H), 6.97–7.00 (m, 6H), 7.04–7.10 (m, 6H), 7.39 (dd, $J = 7.6, 4.8$ Hz, 2H), 7.50 (dd, $J = 4.8, 1.6$ Hz, 2H), 8.24 (dd, $J = 7.6, 1.6$ Hz, 2H), 8.57 (s, 2H), 8.66 (dd, $J = 4.8, 1.6$ Hz, 2H), 8.75 (d, $J = 5.2$ Hz, 2H), 8.80 (dd, $J = 5.2, 1.6$ Hz, 2H). ESI-MS: $m/z = 727.4$ (M + H)⁺. Anal. Calcd for C₄₆H₃₀N₈O₂ (%): C, 76.0; H, 4.2; N, 15.4. Found: C, 76.3; H, 4.4; N, 15.6. IR ν_{\max} (KBr, cm⁻¹): 3429 (br), 1641w, 1597m, 1562m, 1500s, 1455w, 1398s, 1281w, 1236s, 1164w, 1105w, 1045w, 831m, 755m, 621w, 537w.

[{Ru(bpy)₂}₃(μ_3 -L¹)](PF₆)₆: A mixture of L¹ (82 mg, 0.14 mM) and Ru(bpy)₂Cl₂·2H₂O (307 mg, 0.59 mM) in 2-methoxyethanol (100 mL) was heated to 120 °C for 12 h under nitrogen to get a clear deep red solution, then the solvent was evaporated under reduced pressure. The residue was purified twice by column chromatography on alumina, being eluted first with CH₃CN–EtOH (6 : 1, v/v) to remove impurities, then with EtOH to afford [{Ru(bpy)₂}₃(μ_3 -L¹)]Cl₆. This complex was dissolved in minimum amount of water followed by dropwise addition of saturated aqueous NH₄PF₆ until no more precipitate formed. The precipitate was recrystallized from CH₃CN–Et₂O mixture (vapor diffusion method) to afford a red solid. Yield: 136 mg (35.42%). ¹H NMR (400 MHz, DMSO-d₆): $\delta = 5.68$ (s, 4H), 7.44–7.67 (m, 16H), 7.70–7.75 (m, 4H), 7.85–7.97 (m, 4H), 8.08 (d, $J = 7.2$ Hz, 2H), 8.12–8.25 (m, 16H), 8.28 (d, $J = 7.2$ Hz, 2H), 8.52 (s, 2H), 8.67–8.73 (m, 4H), 8.79–8.89 (m, 16H). ESI-MS: $m/z = 750.4$ (M - 3PF₆)³⁺, 526.8 (M - 4PF₆)⁴⁺. Anal. Calcd for C₉₄H₇₀F₃₆N₂₀O₂P₆Ru₃ (%): C, 42.1; H, 2.6; N, 10.4. Found: C, 42.3; H, 2.8; N, 10.6. IR ν_{\max} (KBr, cm⁻¹): 3423 (br), 1608m, 1448m, 1421m, 1242w, 1109m, 844s, 766m, 559s.

[{Ru(bpy)₂}₃(μ_3 -L²)](PF₆)₆: [{Ru(bpy)₂}₃(μ_3 -L²)](PF₆)₆ was prepared by the same procedure as that described for [{Ru(bpy)₂}₃(μ_3 -L¹)](PF₆)₆, except L² (79 mg, 0.11 mM) was used instead of L¹ to react with Ru(bpy)₂Cl₂·2H₂O (226 mg, 0.43 mM). Yield: 113 mg (36.69%) of a red solid. ¹H NMR (400 MHz, DMSO-d₆): $\delta = 5.48$ (s, 4H), 7.09–7.20 (m, 4H), 7.29–7.38 (m, 4H), 7.47–7.52 (m, 4H), 7.54–7.61 (m, 10H), 7.65 (d, $J = 5.2$ Hz, 2H), 7.67 (s, 4H), 7.71–7.74 (m, 4H), 7.81 (d, $J = 6.0$ Hz, 2H), 7.85 (d, $J = 6.0$ Hz, 2H), 8.10 (d, $J = 5.6$ Hz, 2H), 8.14–8.22 (m, 14H), 8.47 (d, $J = 7.2$ Hz, 2H), 8.68 (s, 4H), 8.77–8.82 (m, 16H). ESI-MS: $m/z = 1274.0$ (M - 2PF₆)²⁺, 800.8 (M - 3PF₆)³⁺, 564.2 (M - 4PF₆)⁴⁺. Anal. Calcd for C₁₀₆H₇₈F₃₆N₂₀O₂P₆Ru₃: C, 44.9; H, 2.8; N, 9.9. Found: C, 45.1; H, 2.9; N, 10.1. IR ν_{\max} (KBr, cm⁻¹): 1607 m, 1422 m, 1242w, 1109 m, 1040w, 842s, 763 m, 558s.

[{Ru(bpy)₂}₃(μ_3 -L³)](PF₆)₆: [{Ru(bpy)₂}₃(μ_3 -L³)](PF₆)₆ was prepared by the same procedure as that described for [{Ru(bpy)₂}₃(μ_3 -L¹)](PF₆)₆, except L³ (90 mg, 0.12 mM) was used instead of L¹ to react with Ru(bpy)₂Cl₂·2H₂O (269 mg, 0.52 mM). Yield: 109 mg (30.97%) of a red solid. ¹H NMR (400 MHz, DMSO-d₆): $\delta = 5.45$ (s, 4H), 7.19–7.24 (m, 4H), 7.54–7.63 (m, 16H), 7.73–7.77 (m, 10H), 7.86 (t, $J = 5.6$ Hz, 4H), 8.07 (d, $J = 8.8$ Hz, 2H), 8.16–8.25 (m, 16H), 8.48 (t, $J = 8.0$ Hz, 2H), 8.73 (d, $J = 8.0$ Hz, 4H), 8.79–8.86 (m, 16H). ESI-MS: $m/z = 1273.7$ (M - 2PF₆)²⁺, 800.2 (M - 3PF₆)³⁺. Anal. Calcd for C₁₀₆H₇₈F₃₆N₂₀O₂P₆Ru₃: C, 44.9; H, 2.8; N, 9.9. Found: C, 45.1; H, 2.9; N, 10.1. IR

ν_{\max} (KBr, cm^{-1}): 1607m, 1511m, 1449m, 1422m, 1239m, 1166w, 1047w, 842s, 764s, 557s, 420w.

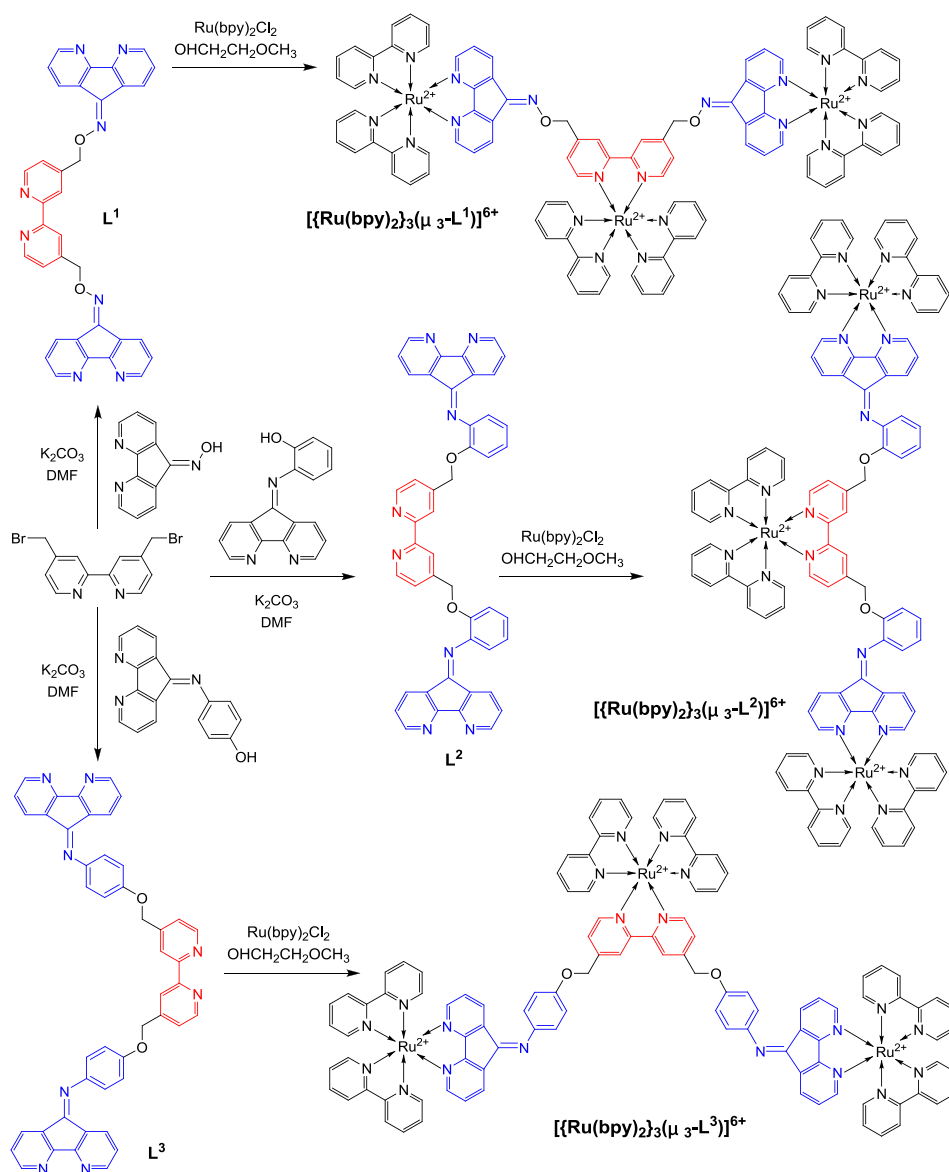
3. Results and discussion

3.1. Synthesis

An outline of the synthesis of the three heterotopic bridging ligands and their Ru(II) complexes is presented in scheme 1. The starting compounds 4,5-diazafluoren-9-oxime, 9-(2-hydroxy)phenylimino-4,5-diazafluorene, and 9-(4-hydroxy)phenylimino-4,5-diazafluorene were synthesized from 4,5-diazafluoren-9-one according to the literature procedure [21, 22]. Heterotopic ligands L^1 , L^2 and L^3 were prepared in good yields by reaction of 4,4'-bis(bromomethyl)-2,2'-bipyridine with 4,5-diazafluoren-9-oxime, 9-(2-hydroxy)phenylimino-4,5-diazafluorene, and 9-(4-hydroxy)phenylimino-4,5-diazafluorene, respectively, in DMF. The three Ru(II) complexes were prepared by refluxing $\text{Ru}(\text{bpy})_2\text{Cl}_2 \cdot 2\text{H}_2\text{O}$ and the ligands in 2-methoxyethanol solution and isolated as their PF_6^- salts. These compounds were characterized by ^1H NMR, ESI-MS, IR, and elemental analysis.

Elemental analysis was consistent with the formation of the three bridging ligands and their trinuclear Ru(II) systems. Rillema and co-workers reported the electronic and ^1H NMR properties of a series of polypyridyl ligands derived from 4,5-diazafluoren-9-one [22]. Due to sp^2 hybridization of the nitrogen (h) in the bridge, the structure of the 4,5-diazafluoren-9-one derivative is asymmetric, the protons in the two pyridine units of each 4,5-diazafluorene group are nonequivalent. As shown for L^1 (figure S1, see online supplemental material at <http://dx.doi.org/10.1080/00958972.2014.994512>), 22 protons are divided into ten groups, the chemical shifts for a, b, and c protons are 8.75, 7.34, and 8.06 ppm, respectively; the chemical shifts for a', b', and c' protons are 8.72, 7.29, and 8.57 ppm, respectively. The calculated molecular weight of L^1 is 574.2. Figure S2 shows the ESI-MS spectrum of L^1 . The main peak at $m/z = 575.3$ is assigned to $(\text{M} + \text{H})^+$ and the other small peak at $m/z = 597.3$ is assigned to $(\text{M} + \text{Na})^+$.

Octahedral metal centers with bidentate ligands generally show stereoisomerism. The number of stereoisomeric possibilities in polynuclear complexes increases exponentially with the number of metal centers. Although the ^1H NMR spectra of some Ru(II) polypyridyl complexes have been clearly described [27, 28], in most cases, the ^1H NMR spectra of polynuclear Ru(II) complexes are complicated. The protons in the two pyridine units of each 4,5-diazafluorene group of the complexes $[\{\text{Ru}(\text{bpy})_2\}_3(\mu_3\text{-L}^{1-3})](\text{PF}_6)_6$ are unequal, therefore, the ^1H NMR spectra of the three complexes are complicated and the assignment of the proton signals is difficult. The structures of the three trinuclear Ru(II) complexes are further established by ESI-MS spectra. This technique has proven to be very helpful for identifying polynuclear transition metal complexes with high molecular masses [29, 30]. The data with the assignments of the peaks are given in the experimental section. Usually, the mass is calculated from a series of multiple charged ions obtained by the successive loss of counter anions. The ESI-MS spectra of the three complexes exhibit some expected peaks due to $[\text{M} - n\text{PF}_6]^{n+}$ cations. Figure S3 shows the ESI-MS spectrum of $[\{\text{Ru}(\text{bpy})_2\}_3(\mu_3\text{-L}^2)](\text{PF}_6)_6$. The main peak at $m/z = 800.8$ is assigned to $(\text{M} - 3\text{PF}_6)^{3+}$ and the other two peaks at $m/z = 564.2$ and 1274.0 are assigned to $(\text{M} - 4\text{PF}_6)^{4+}$ and $(\text{M} - 2\text{PF}_6)^{2+}$, respectively. The measured molecular weights are consistent with expected values.



Scheme 1. Synthesis of L^{1-3} and $[(Ru(bpy)_2)_3(\mu_3-L^{1-3})](PF_6)_6$.

3.2. Molecular orbital calculations of bridging ligands

The compositions and energies of the three bridging ligand orbitals have been obtained to rationalize the spectroscopic and electrochemical results (table 1). Theoretical energy levels of the three ligands have been calculated using Gaussian 09D program at B3LYP/3-21G level. Figure 1 shows the graphical illustrations for the HOMO and the three LUMO of the three ligands. The HOMO of L^1 is centered on the 2,2'-bipyridine portion, whereas the HOMO of L^2 and L^3 are mainly centered on the benzene portion. The LUMO of the three

Table 1. The calculated HOMO and LUMO energies of the three bridging ligands.

Compound	E_{HOMO} (eV)	E_{LUMO} (eV)	$E_{\text{LUMO}+1}$ (eV)	$E_{\text{LUMO}+2}$ (eV)
L ¹	-6.32	-2.38	-1.50	-1.46
L ²	-6.07	-2.50	-1.47	-1.28
L ³	-6.14	-2.58	-1.48	-1.32

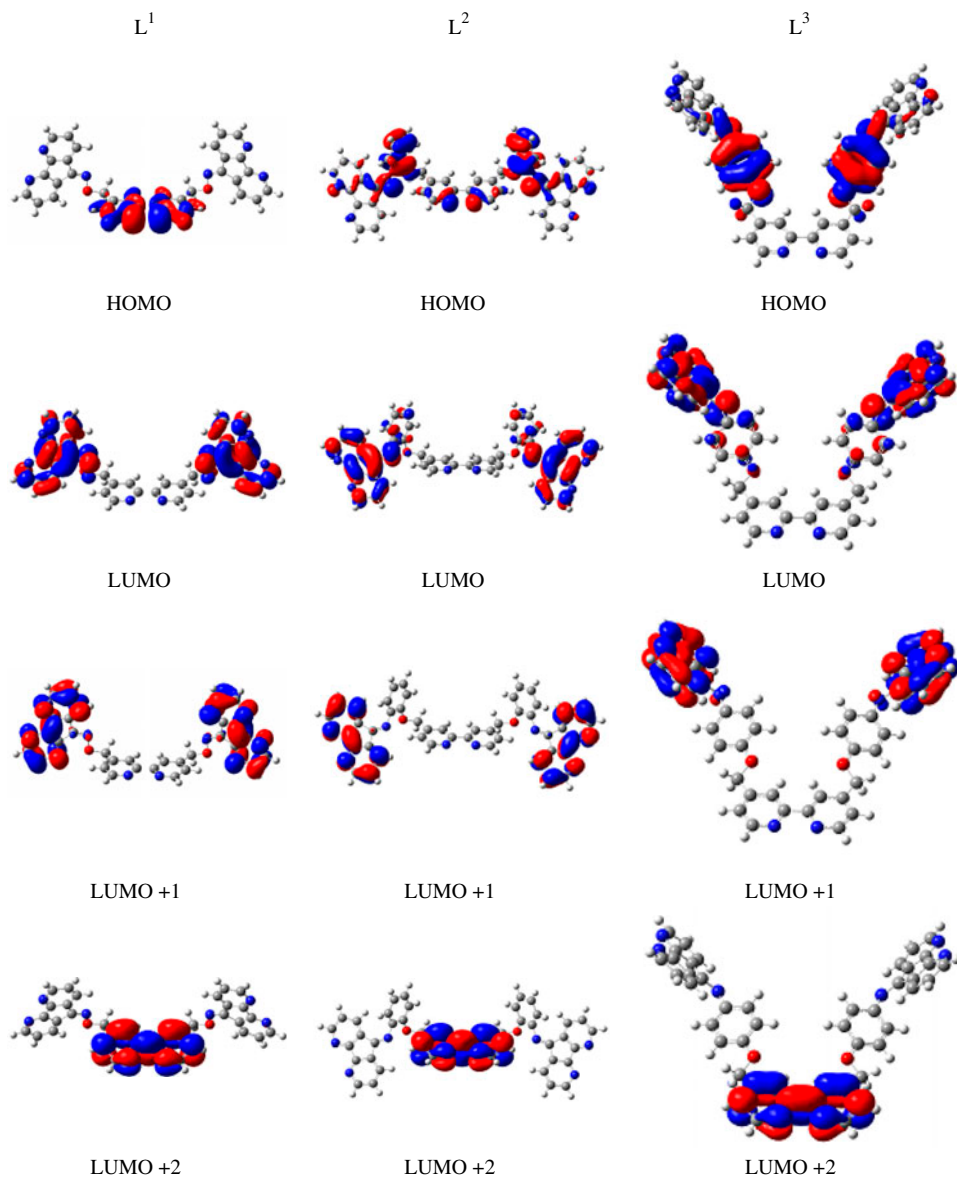


Figure 1. Graphical illustrations for the HOMO and LUMOs of the three bridging ligands.

ligands is centered on 4,5-diazafluoren-9-ylimino. The next vacant LUMO + 1 lying at higher energy is constricted on the 4,5-diazafluorene. The LUMO and LUMO + 1 receive negligible contribution from 2,2'-bipyridine. In contrast, LUMO + 2 is developed on the 2,2'-bipyridine part and with very little electron density on the 4,5-diazafluorene. This simple electronic approach reflects the nonequivalent nature of two coordinating sites on the heterotopic bridging ligands.

3.3. Photophysical and electrochemical behavior of complexes

The UV–vis absorption spectra of the complexes in CH_3CN ($5 \times 10^{-6} \text{ M L}^{-1}$) and ligands in $\text{CHCl}_3\text{--MeOH}$ (1 : 1, v/v) solution (10^{-5} M L^{-1}) are shown in figure 2. The absorption maxima and corresponding molar absorption coefficients are listed in table 2. L^1 shows intraligand $\pi \rightarrow \pi^*$ or $n \rightarrow \pi^*$ transitions at 292 nm with one shoulder at 314 nm; L^2 and L^3 exhibit intraligand $\pi \rightarrow \pi^*$ or $n \rightarrow \pi^*$ transitions at 423, 315, and 283 nm. Assignments of the absorption bands of the three complexes have been made on the basis of the well-documented optical transitions of analogous Ru(II) polypyridyl complexes [31–34]. The UV–vis absorption spectra of the three complexes are dominated by very intense spin-allowed ligand-centered (LC) transitions in the UV region and by intense spin-allowed MLCT transitions in the visible region. The bands at 286 and 240 nm can be assigned to intraligand $\pi \rightarrow \pi^*$ transitions centered on the 2,2'-bipyridine. The lowest energy band at 446 nm is assigned to spin-allowed $d\pi \rightarrow \pi^*$ MLCT transition, which upon intersystem crossing directly produces the triplet MLCT excited state. The $d\pi \rightarrow \pi^*$ transition consists of overlapping $d\pi(\text{Ru}) \rightarrow \pi^*(\text{bpy})$ and $d\pi(\text{Ru}) \rightarrow \pi^*(\text{L})$ components. The three heterotopic ligands contain two kinds of bidentate units with different accepting properties (2,2'-bipyridine and

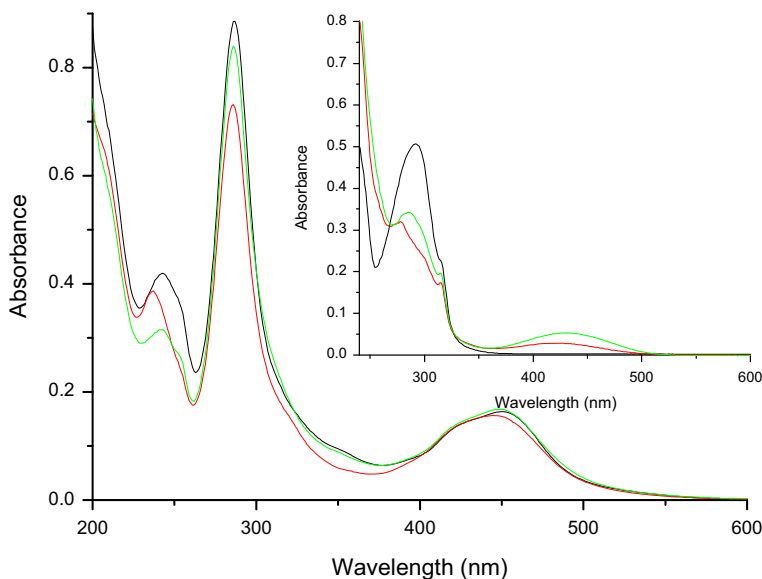


Figure 2. Absorption spectra of complexes ($5 \times 10^{-6} \text{ M L}^{-1}$) $[\{\text{Ru}(\text{bpy})_2\}_3(\mu_3\text{-L}^1)]^{6+}$ (red), $[\{\text{Ru}(\text{bpy})_2\}_3(\mu_3\text{-L}^2)]^{6+}$ (green), and $[\{\text{Ru}(\text{bpy})_2\}_3(\mu_3\text{-L}^3)]^{6+}$ (black) in CH_3CN solution at room temperature; the inset shows absorption spectra of ligands (10^{-5} M L^{-1}) L^1 (black), L^2 (red), and L^3 (green) in $\text{CHCl}_3\text{--MeOH}$ (1 : 1, v/v) solution at room temperature (see <http://dx.doi.org/10.1080/00958972.2014.994512> for color version).

Table 2. Photophysical and electrochemical data of the three bridging ligands and their Ru(II) polypyridyl complexes.

Compound	Absorption λ_{\max} , nm ($10^4 \epsilon$, $M^{-1} \text{ cm}^{-1}$)	Emission ^a		$E_{1/2}$, V (ΔE_p , mV) ^b Oxidation
		λ_{\max} , nm Φ (298 K) τ (ns)	λ_{\max} , nm Φ (77 K) τ (μs)	
L ¹	314 (shoulder) 292 (0.51)			
L ²	419 (0.28) 315 (1.74) 278 (3.20)			
L ³	428 (0.53) 315 (1.96) 286 (3.42)			
$[\{\text{Ru}(\text{bpy})_2\}_3(\mu_3\text{-L}^1)]^{6+}$	445 (3.12) 286 (14.64)	652 (0.014)	657 (0.308)	1.33 (91)
$[\{\text{Ru}(\text{bpy})_2\}_3(\mu_3\text{-L}^2)]^{6+}$	449 (3.36) 286 (16.80) 242 (6.31)	625 (0.016) (672)	645 (0.155) (4.21)	1.31 (116)
$[\{\text{Ru}(\text{bpy})_2\}_3(\mu_3\text{-L}^3)]^{6+}$	450 (3.28) 287 (17.72) 243 (8.39)	626 (0.015) (693)	646 (0.148) (4.45)	1.31 (110)

^aThe emission quantum yields are calculated relative to $\text{Ru}(\text{bpy})_3^{2+}$ ($\Phi_{\text{std}} = 0.062$) in deoxygenated CH_3CN solution at 298 K or relative to $\text{Ru}(\text{bpy})_3^{2+}$ ($\Phi_{\text{std}} = 0.376$) in EtOH–MeOH (4 : 1, v/v) glassy matrix at 77 K; the uncertainty in quantum yields is 15%.

^bOxidation potentials are recorded in 0.1 $M L^{-1}$ TBAP/ CH_3CN and potentials are given vs. SCE, scan rate = 200 mV/s, and ΔE_p is the difference between the anodic and cathodic waves.

4,5-diazafluorene), which results in the appearance of a nonsymmetrical MLCT band. The blue shift observed in going from $[\{\text{Ru}(\text{bpy})_2\}_3(\mu_3\text{-L}^2)]^{6+}$ and $[\{\text{Ru}(\text{bpy})_2\}_3(\mu_3\text{-L}^3)]^{6+}$ to $[\{\text{Ru}(\text{bpy})_2\}_3(\mu_3\text{-L}^1)]^{6+}$ is due to an increase in the energy of LUMO of L¹, causing the $d\pi \rightarrow \pi^*$ transition to occur at higher energy.

The emission spectra of the three Ru(II) complexes have been measured in degassed CH_3CN solution at room temperature and in EtOH–MeOH (4 : 1, v/v) glassy matrix at 77 K, the emission band maxima, emission quantum yields, and emission lifetimes are listed in table 2. Upon excitation into the MLCT band, the three complexes show almost equal emission intensities in CH_3CN solution at room temperature (figure 3). $\text{Ru}(\text{bpy})_3^{2+}$ is a potent light absorber that can be optically excited into the ¹MLCT excited state with UV or visible light to efficiently populate the emissive, long-lived ³MLCT excited state. The ³MLCT state is reasonably long-lived and is thought to be deactivated by three processes: radiative decay k_r , radiationless decay k_{nr} , and thermal population of a higher lying excited state, $k_o \exp(-\Delta E/RT)$. For the last process, the energy of this LF excited state depends on the LF strength. The extensive studies on $\text{Ru}(\text{bpy})_3^{2+}$ have led to the model shown in figure 4 [35–39]. The energy difference (ΔE) between the ³MLCT excited state and LF excited state has been evaluated as 3600 cm^{-1} in water for $\text{Ru}(\text{bpy})_3^{2+}$ [40]. Diazafluorene derivatives are known to be lower than 2,2'-bipyridine in the spectrochemical series [31–34]. Hence, substitution of diazafluorene derivatives for 2,2'-bipyridine results in a decreased LF and therefore, a lower LF excited state energy. Since the ³MLCT excited state is not significantly affected, the values of ΔE for the Ru(II) diimine complexes containing diazafluorene derivatives are substantially lower than the corresponding value for $\text{Ru}(\text{bpy})_3^{2+}$. Consequently, population of the LF state is very efficient for these complexes at room temperature and they are essentially non-emissive at room temperature.

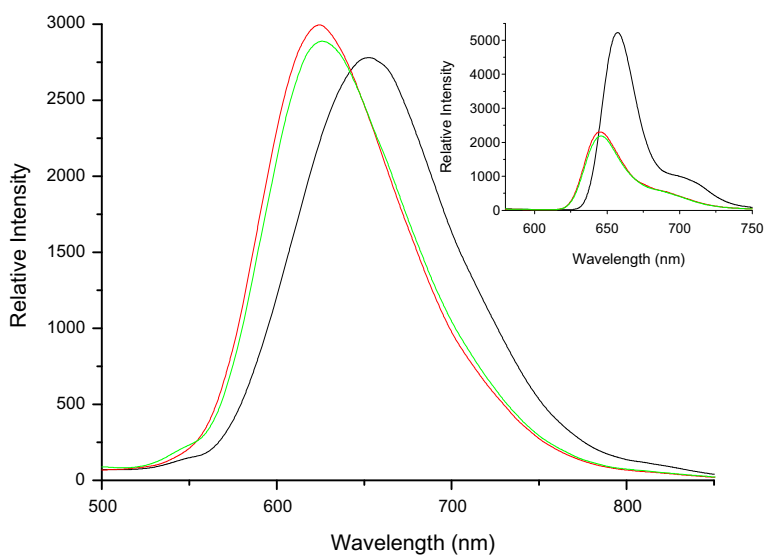


Figure 3. Emission spectra of $[\{\text{Ru}(\text{bpy})_2\}_3(\mu_3\text{-L}^1)]^{6+}$ (black), $[\{\text{Ru}(\text{bpy})_2\}_3(\mu_3\text{-L}^2)]^{6+}$ (red), and $[\{\text{Ru}(\text{bpy})_2\}_3(\mu_3\text{-L}^3)]^{6+}$ (green) in CH_3CN solution at room temperature; (Inset) $[\{\text{Ru}(\text{bpy})_2\}_3(\mu_3\text{-L}^1)]^{6+}$ (black), $[\{\text{Ru}(\text{bpy})_2\}_3(\mu_3\text{-L}^2)]^{6+}$ (red), and $[\{\text{Ru}(\text{bpy})_2\}_3(\mu_3\text{-L}^3)]^{6+}$ (green) in EtOH–MeOH (4 : 1, v/v) glassy matrix at 77 K (see <http://dx.doi.org/10.1080/00958972.2014.994512> for color version).

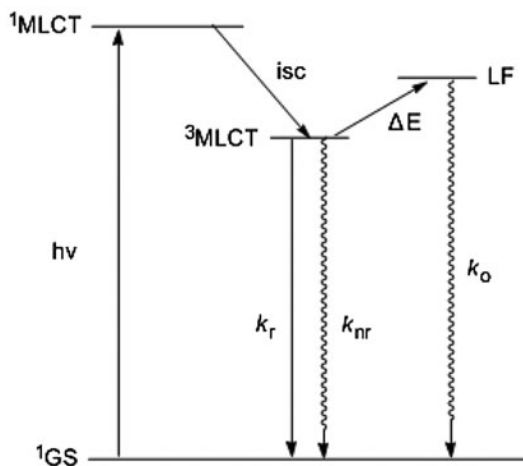


Figure 4. Energy state diagram based on the Crosby–Meyer model.

$[\{\text{Ru}(\text{bpy})_2\}_3(\mu_3\text{-L}^1)]^{6+}$, $[\{\text{Ru}(\text{bpy})_2\}_3(\mu_3\text{-L}^2)]^{6+}$, and $[\{\text{Ru}(\text{bpy})_2\}_3(\mu_3\text{-L}^3)]^{6+}$ all have three Ru(II) polypyridine subunits. Based on the above LF theory, two Ru(II) polypyridine subunits containing 4,5-diazafluorene are non-emissive, so the three complexes have only one efficient emission subunit $\text{Ru}(\text{bpy})_3^{2++}$ and exhibit similar emission intensities in CH_3CN solution at room temperature. In addition, the same conclusion is supported by the calculated result with the equations $k_r = \Phi/\tau$ and $k_{nr} = 1/\tau - k_r$. The calculated rates of k_r and k_{nr} processes of the three complexes are close in CH_3CN solution at room temperature

(k_r and k_{nr} for $[\{\text{Ru}(\text{bpy})_2\}_3(\mu_3\text{-L}^1)]^{6+}$: 1.95×10^4 and 1.37×10^6 ; k_r and k_{nr} for $[\{\text{Ru}(\text{bpy})_2\}_3(\mu_3\text{-L}^2)]^{6+}$: 2.38×10^4 and 1.46×10^6 ; k_r and k_{nr} for $[\{\text{Ru}(\text{bpy})_2\}_3(\mu_3\text{-L}^3)]^{6+}$: 2.16×10^4 and 1.42×10^6).

The energy transfer of Ru(II) polypyridine complexes containing 4,5-diazafluorene is inhibited at 77 K, the three complexes show vibrational components similar to that of $\text{Ru}(\text{bpy})_3^{2+}$ in EtOH–MeOH (4 : 1, v/v) glassy matrix at 77 K (figure 3) [31–34], however, the emission intensities of $[\{\text{Ru}(\text{bpy})_2\}_3(\mu_3\text{-L}^2)]^{6+}$ and $[\{\text{Ru}(\text{bpy})_2\}_3(\mu_3\text{-L}^3)]^{6+}$ are weaker than that of $[\{\text{Ru}(\text{bpy})_2\}_3(\mu_3\text{-L}^1)]^{6+}$ in EtOH–MeOH glassy matrix. The rate constant of k_r of $[\{\text{Ru}(\text{bpy})_2\}_3(\mu_3\text{-L}^1)]^{6+}$ is larger than those of $[\{\text{Ru}(\text{bpy})_2\}_3(\mu_3\text{-L}^2)]^{6+}$ and $[\{\text{Ru}(\text{bpy})_2\}_3(\mu_3\text{-L}^3)]^{6+}$ (k_r for $[\{\text{Ru}(\text{bpy})_2\}_3(\mu_3\text{-L}^1)]^{6+}$, $[\{\text{Ru}(\text{bpy})_2\}_3(\mu_3\text{-L}^2)]^{6+}$, and $[\{\text{Ru}(\text{bpy})_2\}_3(\mu_3\text{-L}^3)]^{6+}$: 6.53×10^4 , 3.68×10^4 and 3.32×10^4).

The electrochemical properties of the three complexes have been studied by cyclic voltammetry and differential pulse voltammetry, in acetonitrile solutions, with 0.1 M L^{-1} TBAP as supporting electrolyte (table 2). $[\{\text{Ru}(\text{bpy})_2\}_3(\mu_3\text{-L}^1)]^{6+}$ exhibits a Ru(II)-centered quasi-reversible oxidation wave at $E(\text{onset})^{\text{ox}} = 1.33 \text{ V vs. SCE}$ for the $\text{Ru}^{\text{II/III}}$ couple (figure 5). This potential is slightly more negative (by about 60 mV) than that of the parent complex $[(\text{bpy})_2\text{Ru}(\text{dafone})]^{2+}$ [32], but slightly more positive (by about 60 mV) than that of $\text{Ru}(\text{bpy})_3^{2+}$ (+1.28 V vs. SCE) [41], which indicates that L^1 is a stronger π -acceptor than 2,2'-bipyridine but a weaker π -acceptor than dafone. $[\{\text{Ru}(\text{bpy})_2\}_3(\mu_3\text{-L}^1)]^{6+}$ has three Ru(II) centers; two of one type of coordination environment, while the other one is different. The complex shows a single wave in cyclic voltammetry and a single peak without broadening in differential pulse voltammetry, which indicates that the small redox potential difference caused by different coordination environments is not resolved by electrochemical means. The $\text{Ru}^{\text{II/III}}$ couple of $[\{\text{Ru}(\text{bpy})_2\}_3(\mu_3\text{-L}^1)]^{6+}$ is slightly more positive (by about 20 mV) than that of $[\{\text{Ru}(\text{bpy})_2\}_3(\mu_3\text{-L}^2)]^{6+}$ and $[\{\text{Ru}(\text{bpy})_2\}_3(\mu_3\text{-L}^3)]^{6+}$. This also suggests that the better σ^* acceptor character of L^1 stabilizes the ruthenium-based HOMO, rendering oxidation of the metal more difficult.

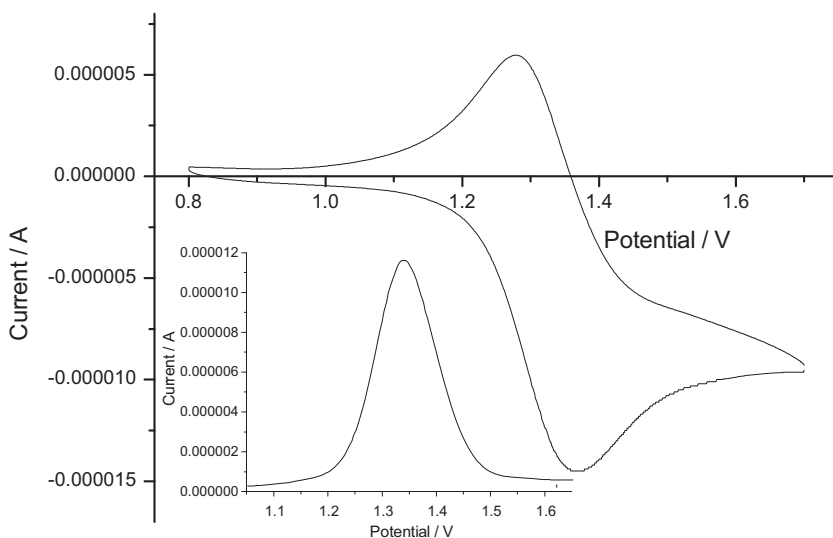


Figure 5. Cyclic voltammetry and differential pulse voltammetry of $[\{\text{Ru}(\text{bpy})_2\}_3(\mu_3\text{-L}^1)]^{6+}$ ($5 \times 10^{-4} \text{ M L}^{-1}$) in CH_3CN .

Table 3. The estimated HOMO and LUMO energies and energy gaps of the three complexes.

Complex	$E(\text{onset})^{\text{ox}}$ (V)	E_{HOMO} (eV)	E_{LUMO} (eV)	E_{g} (eV)
$[\{\text{Ru}(\text{bpy})_2\}_3(\mu_3\text{-L}^1)]^{6+}$	1.33	-6.07	-3.28	2.79
$[\{\text{Ru}(\text{bpy})_2\}_3(\mu_3\text{-L}^2)]^{6+}$	1.31	-6.05	-3.28	2.77
$[\{\text{Ru}(\text{bpy})_2\}_3(\mu_3\text{-L}^3)]^{6+}$	1.31	-6.05	-3.27	2.78

Extended Hückel calculations toward the three trinuclear complexes were precluded by program limitations concerning the number of atoms. From the onset anodic peak potential for the oxidation process $E(\text{onset})^{\text{ox}}$ and the UV-vis absorption spectra, HOMO and LUMO energy levels of the three Ru(II) complexes were estimated by taking 4.74 eV for SCE with respect to the vacuum level according to the following formulas: $E_{\text{HOMO}} = -4.74 - E(\text{onset})^{\text{ox}}$ and $E_{\text{LUMO}} = E_{\text{HOMO}} + E_{\text{g}}$ [42, 43]. E_{g} is the band gap energy between the HOMO and LUMO energy levels and calculated using the formula $E_{\text{g}} = hc/\lambda$ [42, 43], where λ is the wavelength in nm of the MLCT band. These calculations give the HOMO and LUMO energy levels of about -6.06 and -3.28 eV, respectively, for the three complexes (table 3). These calculations provide a valuable first approximation of the orbital energies.

4. Conclusion

Three heterotopic ligands consisting of 2,2'-bipyridine and 4,5-diazafluorene have been synthesized and characterized. 4,5-Diazafluorene is lower than 2,2'-bipyridine in the spectrochemical series which translates into an energetic lowering of any LF states while leaving MLCT states nearly unchanged for Ru(II) diimine complexes. The photophysical and electrochemical properties of the three complexes are different from those of $\text{Ru}(\text{bpy})_3^{2+}$ and $\text{Ru}(\text{phen})_3^{2+}$ due to the different electronic nature of the bridging ligands. Emission behaviors of the three complexes are similar in CH_3CN solution at room temperature, but different in EtOH-MeOH (4 : 1, v/v) glassy matrix at 77 K. Cyclic voltammetry and differential pulse voltammetry of the three complexes show one single Ru(II)-centered oxidation wave without broadening. An interaction of a few reciprocal centimeters (which cannot be noticed in spectroscopic and electrochemical experiments) is sufficient to cause fast inter-component electron or energy transfer processes [44-46], so the three complexes have potential applications in photo-induced electron or energy transfer.

Funding

We are grateful to the National Natural Science Foundation of China [grant number 21261019] and the Yunnan Provincial Science and Technology Department [grant number 2010ZC148] for financial support.

References

- [1] M. Natali, S. Campagna, F. Scandola. *Chem. Soc. Rev.*, **43**, 4005 (2014). doi:10.1039/C3CS60463B.
- [2] J.R. Robinson, Z. Gordon, C.H. Booth, P.J. Carroll, P.J. Walsh, E.J. Schelter. *J. Am. Chem. Soc.*, **135**, 19016 (2013).
- [3] S. Liatard, J. Chauvin, D. Jouvenot, F. Loiseau, A. Deronzier. *J. Phys. Chem. C*, **117**, 20431 (2013).
- [4] D. Maity, C. Bhaumik, S. Karmakar, S. Baitalik. *Inorg. Chem.*, **52**, 7933 (2013).

- [5] C. Herrero, A. Quaranta, S.E. Ghachtouli, B. Vauzeilles, W. Leibl, A. Aukauloo. *Phys. Chem. Chem. Phys.*, **16**, 12067 (2014). doi:10.1039/C3CP54946A.
- [6] G.E. Pieslinger, P. Albores, L.D. Slep, B.J. Coe, C.J. Timpson, L.M. Baraldo. *Inorg. Chem.*, **52**, 2906 (2013).
- [7] B.H. Farnum, Z.A. Morseth, A.M. Lapidés, A.J. Rieth, P.G. Hoertz, M.K. Brennaman, J.M. Papanikolas, T.J. Meyer. *J. Am. Chem. Soc.*, **136**, 2208 (2014).
- [8] S. Das, S. Karmakar, D. Saha, S. Baitalik. *Inorg. Chem.*, **52**, 6860 (2013).
- [9] W. Chen, F.N. Rein, B.L. Scott, R.C. Rocha. *Chem. Eur. J.*, **17**, 5595 (2011).
- [10] D. Schallenberg, A. Neubauer, E. Erdmann, M. Tänzler, A. Villinger, S. Lochbrunner, W.W. Seidel. *Inorg. Chem.*, **53**, 8859 (2014).
- [11] S. Shi, J. Liu, T. Yao, X. Geng, L. Jiang, Q. Yang, L. Cheng, L. Ji. *Inorg. Chem.*, **47**, 2910 (2008).
- [12] T.L. Easun, W.Z. Alsindi, N. Deppermann, M. Towrie, K.L. Ronayne, X.Z. Sun, M.D. Ward, M.W. George. *Inorg. Chem.*, **48**, 8759 (2009).
- [13] M. Gueffi, F. Puntoriero, A. Arrigo, S. Serroni, M. Cifelli, G. Denti. *Inorg. Chim. Acta*, **398**, 19 (2013).
- [14] M. Borgstrom, S. Ott, R. Lomoth, J. Bergquist, L. Hammarstrom, O. Johansson. *Inorg. Chem.*, **45**, 4820 (2006).
- [15] H. Chao, Z.R. Qiu, L.R. Cai, H. Zhang, X.Y. Li, K.S. Wong, L.N. Ji. *Inorg. Chem.*, **42**, 8823 (2003).
- [16] E.C. Constable, E. Figgemeier, C.E. Housecroft, J. Olsson, Y.C. Zimmermann. *Dalton Trans.*, **13**, 1918 (2004).
- [17] E. Coronado, P. Gavina, S. Tatay, R. Groarke, J.G. Vos. *Inorg. Chem.*, **49**, 6897 (2010).
- [18] J. Leveque, B. Elias, C. Moucheron, A. Kirsch-De Mesmaeker. *Inorg. Chem.*, **44**, 393 (2005).
- [19] A. Valore, M. Balordi, A. Colombo, C. Dragonetti, S. Righetto, D. Roberto, R. Ugo, T. Benincori, G. Rampinini, F. Sannicolò, F. Demartine. *Dalton Trans.*, **39**, 10314 (2010).
- [20] H. Jiang, D. Song. *Organometallics*, **27**, 3587 (2008).
- [21] L.J. Henderson, F.R. Fronczek, W.R. Cherry. *J. Am. Chem. Soc.*, **106**, 5876 (1984).
- [22] Y. Wang, D.P. Rillema. *Tetrahedron*, **53**, 12377 (1997).
- [23] I.G. Gauthier, F. Odobel, M. Alebbi, R. Argazzi, E. Costa, C.A. Bignozzi, P. Qu, G.J. Meyer. *Inorg. Chem.*, **40**, 6073 (2002).
- [24] B.P. Sullivan, D.J. Salmon, T.J. Meyer. *Inorg. Chem.*, **17**, 3334 (1978).
- [25] E. Amouyal, A. Homsí, J.C. Chambron, J.P. Sauvage. *J. Chem. Soc., Dalton Trans.*, 1841 (1990).
- [26] R.J. Watts, G.A. Crosby. *J. Am. Chem. Soc.*, **94**, 2606 (1972).
- [27] T.D. Pilz, N. Rockstroh, S. Rau. *J. Coord. Chem.*, **63**, 2727 (2010).
- [28] B. Elias, L. Herman, C. Moucheron, A.K. Mesmaeker. *Inorg. Chem.*, **46**, 4979 (2007).
- [29] S. Maji, B. Sarkar, M. Patra, A.K. Das, S.M. Mobin, W. Kaim, G.K. Lahiri. *Inorg. Chem.*, **47**, 3218 (2008).
- [30] N.G. Tsierkezos, U. Ritter, A.I. Philippopoulos, D. Schröder. *J. Coord. Chem.*, **63**, 3517 (2010).
- [31] S. Karlsson, J. Modin, H.C. Becker, L. Hammarström, H. Grennberg. *Inorg. Chem.*, **47**, 7286 (2008).
- [32] Y. Wang, W.J. Perez, G.Y. Zheng, D.P. Rillema. *Inorg. Chem.*, **37**, 2051 (1998).
- [33] Y. Wang, W.J. Perez, G.Y. Zheng, D.P. Rillema. *Inorg. Chem.*, **37**, 2227 (1998).
- [34] B.W.K. Chu, V.W.W. Yam. *Inorg. Chem.*, **40**, 3324 (2001).
- [35] G.D. Hager, G.A. Crosby. *J. Am. Chem. Soc.*, **97**, 7031 (1975).
- [36] G.D. Hager, R.J. Watts, G.A. Crosby. *J. Am. Chem. Soc.*, **97**, 7037 (1975).
- [37] K.W. Hipps, G.A. Crosby. *J. Am. Chem. Soc.*, **97**, 7042 (1975).
- [38] T.J. Meyer. *Pure Appl. Chem.*, **62**, 1003 (1990).
- [39] F. Barigelletti, P. Belser, A. von Zelewsky, A. Juris, V. Balzani. *J. Phys. Chem.*, **90**, 5190 (1986).
- [40] J. Van Houten, R.J. Watts. *J. Am. Chem. Soc.*, **98**, 4803 (1976).
- [41] L.J. Charbonnière, R.F. Ziessel, C.A. Sams. *Inorg. Chem.*, **42**, 3466 (2003).
- [42] Y. Wang, A. Suna, W. Mahler, R. Kasowski. *J. Chem. Phys.*, **87**, 7315 (1987).
- [43] Y.Y. Lu, C.C. Ju, D. Guo, Z.B. Deng, K.Z. Wang. *J. Phys. Chem. C*, **111**, 5211 (2007).
- [44] L. De Cola, V. Balzani, F. Barigelletti, L. Flamigni, P. Belser, A.V. Zelewsky, M. Frank, F. Vögtle. *Inorg. Chem.*, **32**, 5228 (1993).
- [45] P. Cai, M. Li, C. Duan, F. Lu, D. Guo, Q. Meng. *New J. Chem.*, **29**, 1011 (2005).
- [46] R.T.F. Jukes, B. Bozic, P. Belser, L. De Cola, F. Hartl. *Inorg. Chem.*, **48**, 1711 (2009).